

Bimorph deformable mirror design

S.G. Lipson, E.N. Ribak, C. Schwartz

Department of Physics, Technion – Israel Institute of Technology,
Haifa 32000, ISRAEL

ABSTRACT

We describe the applicability of wave front correction by using a bimorph mirror in conjunction with a curvature sensor. We use Zernike polynomials to describe analytically the quality of the correction for atmospheric turbulence. The match is limited by boundary conditions of the mirror and by the discreteness of the electrodes. The correction is limited by coupling of lower and higher order Zernike polynomials and necessitates an interfacing computer between the wave front sensor and the bimorph mirror.

1. INTRODUCTION

The bimorph mirror as a wavefront corrector has a response in which its curvature is directly proportional to the applied voltage. Its form is therefore a solution of Poisson's equation. This feature offers, *prima facie*, the advantage that it can be coupled directly to a curvature sensor, possible without an intermediate computer. This paper explores this concept briefly; further details are given in Ref. 1.

The solution of the Poisson equation, and therefore the duplication of the wave front is, however, possible only if suitable boundary conditions are applied. We shall examine two practical aspects in particular:

- a. The possibility of applying boundary conditions by using only the central area of a larger bimorph mirror as the optical aperture.
- b. The use of discrete electrodes which does not allow the application of a continuous voltage distribution.

2. BIMORPH MIRROR

The bimorph mirror in which we are interested is made of two thin layers bonded together². One is made of a piezoelectric material, for example lead-zirconium-titanate – PZT, (which from now on will be used to indicate all similar materials) and the other is made of an opti-

cally polished material (e.g. glass or silicon). We assume that the bonding is ideal – meaning that the adhesive is of negligible thickness and it does not relieve any shearing stresses. A thin conducting film deposited between the two layers acts as a common electrode and the voltage is distributed via electrodes on the back of the PZT (see Fig. 1).

When voltage is applied to the mirror the transverse piezoelectric effect leads to a variation in the area of the PZT. The other layer of the mirror does not react and so spherical bending occurs, much like the linear bending of a bimetallic strip under a temperature variation. The thickness variation is small compared to the area effect.

The PZT layer does not have to be made from a continuous sheet. It can be composed from smaller elements which are much easier to produce. The electrodes can be made to be contiguous, if they are square or hexagonal. Spaces can be left between the electrodes, and spaces will also occur if the electrodes are round. The electrodes cause local bending over their area, whereas areas between the electrodes, if not fully contiguous, take a shape caused by their bent boundaries.

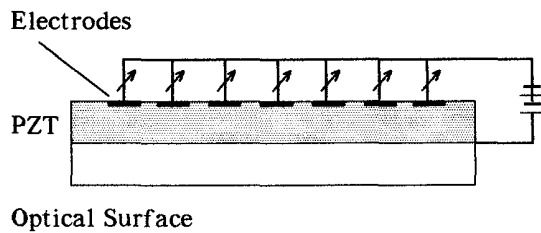


Figure 1. Schematic drawing of a bimorph mirror. A different voltage can be applied to each electrode to control the local curvature. The PZT can be made of a mosaic of elements and not a continuous one.

3. VOLTAGE RESPONSE

A bimorph mirror responds to a voltage distribution applied to it according to the following differential equation⁴, subjected to appropriate boundary conditions:

$$\nabla^4 z = -A \nabla^2 V . \quad (1)$$

$z = z(r, \theta)$ is the deflection of the mirror surface, $V = V(r, \theta)$ is the voltage distribution and A is a constant related to the geometrical, mechanical and piezoelectric properties of the mirror. This equation can be compared to the equation governing the bending of a thin plate under load³. If we assume boundary conditions of a simple support, that is, $z=0$ on the edge with no external moments, we get

$$\nabla^2 z(x, y) = -A V(x, y) \quad (5) \quad (2)$$

This differential equation, the Poisson equation, was discussed by Kokorowsky³ and is equivalent to the equation of a membrane. The equation governing the deformation of the bimorph mirror clearly shows that the local Laplacian of the mirror surface is proportional to the local voltage. The solution of a Poisson equation with boundary condition ($z=0$) on a circle of radius R is⁵

$$z(r, \theta) = \frac{1}{2\pi} \int_0^{2\pi} d\phi \int_0^r \rho d\rho \left[\ln\left(\frac{R}{r}\right) - \sum_{k=1}^{\infty} \frac{1}{k} \left(\frac{\rho^k r^k}{R^{2k}} - \frac{\rho^k}{r^k} \right) \cos k(\phi - \theta) \right] f(\rho, \phi) +$$

$$\frac{1}{2\pi} \int_0^{2\pi} d\phi \int_r^R \rho d\rho \left[\ln\left(\frac{R}{\rho}\right) - \sum_{k=1}^{\infty} \frac{1}{k} \left(\frac{\rho^k r^k}{R^{2k}} - \frac{r^k}{\rho^k} \right) \cos k(\phi - \theta) \right] f(\rho, \phi) . \quad (3)$$

Applying a constant voltage over the entire mirror leads to a spherical surface of the form:

$$z(r) = \frac{A}{4} (R^2 - r^2) . \quad (4)$$

Using the analogy to a bimetallic plate we can derive an expression for A using the solutions for the bending of a round bimetallic plate⁶:

$$A = \frac{12 d_{13} (t_1 + t_2)}{t_1^3 k} \quad (5)$$

$$k = 4 + 6 \left(\frac{t_2}{t_1} \right) + 4 \left(\frac{t_2}{t_1} \right)^2 + \frac{E_2 t_2^3 (1 - \nu_1)}{E_1 t_1^3 (1 - \nu_2)} + \frac{E_1 t_1 (1 - \nu_2)}{E_2 t_2 (1 - \nu_1)} . \quad (6)$$

t is the thickness, E is the Young modulus, and ν is the Poisson ratio. Subscript 1 stands for the PZT and subscript 2 stands for the inert material. d_{13} is the transverse piezoelectric coefficient. In general $\nu_1 \approx \nu_2 \approx 0.3$. In a simple case we take $t_1 \approx t_2 = t$ and $E_1 \approx E_2$ and get:

$$A \approx 1.5 \frac{d_{13}}{t^2} \quad (7)$$

The thermomechanical analogy can be carried further and numerical calculations using thermo-mechanical software based on finite elements have been demonstrated⁷.

4. COUPLING THE BIMORPH MIRROR AND A CURVATURE SENSOR

4.1. Rigorous treatment of the mirror-sensor coupling

Let us now assume we have a wave front curvature sensor as proposed by Roddier⁸ (actually a Laplacian sensor) which is directly coupled to the mirror without any computational stage as was originally proposed by the Roddiers. Curvature sensing is done by subtracting images taken in two planes in front and behind the focal plane. We show now that such direct coupling leads to extra correction errors which unfortunately cannot be eliminated without the use of an intermediate computer. In the following we ignore any sensor noise considerations.

The voltage distribution which is the output of the curvature sensor is

$$A V = \nabla^2 W + \delta(\rho - a) \frac{\partial W}{\partial \rho} \quad \text{when } \rho \leq a, \text{ and otherwise } 0. \quad (8)$$

where $W = W(r, \theta)$ is the measured wave front surface and a is the radius of the optical aperture. We shall apply this voltage distribution to the mirror and assume that we only use a small central area for the actual correction, that is, $a \ll R$. In this way we shall try to deal with the boundary conditions problem⁸. Here we also assume that we can apply a continuous voltage distribution. We include in A all uniform amplification factors between the sensor and the mirror.

The general solution of the Poisson equation (Eq. 2), using Eq. 8, is

$$z(\bar{r}) = \frac{1}{4\pi} \int V(\bar{\rho}) G(\bar{r}/\bar{\rho}) d^2\rho + \frac{1}{4\pi} \int_c \left\{ G(\bar{r}/\rho) \frac{\partial W}{\partial \rho} \Big|_{\rho=a} - W(a) \frac{\partial G}{\partial \rho} \Big|_{\rho=a} \right\} dl \quad (9)$$

where $G(\bar{r}/\bar{\rho})$ is a suitable Green's function

The curvature sensor supplies us with Neumann boundary conditions. In order to get a valid solution (up to an additive constant related to the mean deflection on the boundary) the Green's function must comply with the condition:

$$\frac{\partial G}{\partial \rho} \Big|_{\rho=a} = \text{const.} \quad (10)$$

The Green's function embedded in Eq. 13 has the form⁵ (in polar coordinates):

$$G(\bar{r}/\bar{\rho}) = \begin{cases} -2 \ln(r) + 2 \sum_{k=1}^{\infty} \frac{1}{k} \left(\frac{\rho}{r}\right)^k \cos [k(\phi-\theta)] & r > \rho \\ -2 \ln(\rho) + 2 \sum_{k=1}^{\infty} \frac{1}{k} \left(\frac{r}{\rho}\right)^k \cos [k(\phi-\theta)] & r < \rho \end{cases} \quad (11)$$

This function has a radial derivative at the edge which does not comply with Eq. 10. Therefore the mirror surface duplicates the wave front surface up to a "mismatch" term

$$\frac{1}{2\pi} \sum_{k=1}^{\infty} \left(\frac{r}{a}\right)^k \int_0^{2\pi} d\phi \cos[k(\phi-\theta)] z(a, \phi) \quad (12)$$

This form of the mismatch calls for the use of the Zernike polynomials expansion of aberrations. The Zernike polynomials are a set of orthonormal functions in the unit circle which are very suitable for the analysis of optical problems⁹. Their application to the problems of atmospheric propagation and adaptive optics was described in many papers¹⁰⁻¹². In this work we follow the notation and normalization convention introduced by Noll¹⁰; n stands for the radial index and m for the azimuthal index of the polynomials.

If we introduce a wave front of the form:

$$\Psi(r, \theta) = \sum_{j=1}^{\infty} a_j Z_j(r, \theta) \quad (13)$$

we can see that the isotropic (that is, of azimuthal order, $m=0$) aberrations are fully corrected. This makes sense, since our boundary conditions for the entire mirror ($z=0$) are also isotropic. The aberrations of an higher azimuthal order induce a disturbance term of the form

$$\frac{1}{2\pi} \sum_k \int_0^{2\pi} d\phi r'^k \cos[k(\phi-\theta)] \cos(m\phi) \sqrt{2(n+1)} \quad (14)$$

for Z_{even} and with $\sin(m\phi)$ replacing $\cos(m\phi)$ in Z_{odd} . The normalized radial coordinate is $r' \equiv r/a$. The result of the integral (19) is:

$$\sqrt{\frac{(n+1)}{2}} r'^m \cos(m\theta). \quad (15)$$

A correction of an aberration of an azimuthal order m leaves a residual aberration of the lowest radial order for that azimuthal order (for $m=1$ tilt, for $m=2$ astigmatism and so on) with a factor related to the corrected term radial order. This effect was detected computationally previously¹⁴ but was not explained analytically.

We can write the "correcting wave-front" for the m th azimuthal order

$$\Phi_c^{(m)} = \sum_{j=i}^{\infty} a_j (Z_j^{(m)} + k_j Z_i^{(m)}) \quad (16)$$

where $Z_i^{(m)}$ is the Zernike polynomial of the aberration of the lowest radial order for the azimuthal order m (which is equal to m) and $k_j = \frac{1}{2} \sqrt{\frac{n+1}{m+1}}$ for $m > 0$ and $k_j = \sqrt{\frac{n+1}{2}}$ for $m=0$. The residual mean squared error is

$$\epsilon^2 \equiv \int d^2\rho \langle [\Psi - \Phi_c]^2 \rangle w(\rho) \quad (17)$$

The angular brackets denote the ensemble average over turbulence degraded wave fronts and $w(\rho)$ is the aperture function. The result is:

$$\epsilon^2 = \langle \Psi^2 \rangle - \sum_j \langle |a_j|^2 \rangle + \sum_{j,j'} \langle a_j a_{j'}^* \rangle k_j k_{j'} \quad (18)$$

$\langle \Psi \rangle$, the average of the wave front phase, is taken to be zero.

The terms included in the above sum can be calculated using the formulas derived by Noll¹⁰. Now we assume that the input wave front is degraded by atmospheric turbulence exhibiting Kolmogorov power spectrum. We first assume an open-loop correction scheme, where we sense the wave front and then correct it. A better approach is a closed-loop operation, where the sensing is done on the wave front after correction, which provides the deviations from the required wave front. The result (with no overall tilt correction) is:

$$\epsilon^2 \approx 0.25 (D/r_0)^{5/3}. \quad (19)$$

The computation was done up to the fourth azimuthal order and hence the approximation. $D = 2a$ is the diameter of the optical aperture and r_0 is the turbulence coherence length defined by Fried¹³. The above result is worse than just overall tilt correction, which is $0.134 (D/r_0)^{5/3}$, but

if we remove overall tilt separately the error reduces to

$$\epsilon^2 \approx 0.049 (D/r_0)^{5/3} \quad (20)$$

which is dramatically better. If we now consider a closed loop operation and assume that the control loop is much faster than the turbulence coherence time (~ 10 msec at $0.5 \mu\text{m}$) then the residual aberrations will be eliminated within the coherence time. If the feedback loop is not fast enough then the results for the open-loop operation (Eq. 26) are a good approximation.

The above results are obtained for an ideal sensor-mirror combination for which the Laplacian of the wave front can be sensed continuously, and the measured voltages applied continuously over the mirror surface. This is impossible in practice, and as we shall see later on the discreteness in sensing and voltage application introduces errors that cannot be ignored.

Let us now consider the error that results from the finite size of the mirror. There are two aberration terms. The first is

$$\frac{1}{2\pi} \int_0^{2\pi} d\phi \int_0^a \rho d\rho \left[\sum_{k=1}^{\infty} \frac{1}{k} \left(\frac{\rho r}{a^2} \right)^k \cos k(\phi - \theta) \right] \nabla^2 W(\rho, \phi) . \quad (21)$$

W is again the measured wave front error. This term does not contribute to the lowest radial order for each azimuthal frequency since their Laplacian is zero.

A more substantial term (which couples high terms with low terms) is

$$\frac{1}{2\pi} \int_0^{2\pi} d\phi a \left[\sum_{k=1}^{\infty} \frac{1}{k} \left(\frac{\rho r}{R^2} \right)^k \cos k(\phi - \theta) \right] \left. \frac{\partial W}{\partial \rho} \right|_{\rho=a} \quad (22)$$

This error, as well as the errors we described earlier, can be dealt with if we abandon the direct coupling between the curvature sensor and the bimorph mirror and add a computational stage. In this stage we determine (by solving numerically the Poisson equation) the value of the deflection on the boundary and therefore can compute a voltage distribution that should be applied in order to compensate for the errors given in Eqs. 14 and 22 (we neglect the error term of Eq. 21).

One should take into consideration the practical limitations on the applied voltage: the maximum voltage that can be applied to the PZT without depoling it is of the order of 500 to 1000 V/mm. This voltage corresponds to a maximum curvature which depends on the actual parameters of the bimorph elements. The low aberrations would carry the largest amplitudes, so their correction might reach the maximum voltage. In this case the demands on the applied voltage can

be somewhat alleviated if we use the area of the bimorph mirror outside the optical aperture¹⁵. For example let us consider the error introduced by tilt due to the finite size of the mirror:

$$a_2 \frac{1}{2} \left(\frac{a}{R} \right)^2 r \cos(\theta) \quad (23)$$

a_2 is the tilt (Z_2) expansion coefficient.

This error can be compensated by applying a voltage distribution on the edge of the optical aperture which is proportional to $a_2 (a/R)^2$. Outside the optical aperture we can apply the voltage on a circle of radius ka with a drop of the required voltage by a factor of k^{-2} .

We should note that if we do add a computational phase the curvature sensor loses some of its charm and we can use a conventional slope sensor (like the Hartmann-Shack sensor), even though its performance is less efficient¹⁵. The slope information can be used to derive both the wave front and its Laplacian.

We have assumed that the mirror is fixed on its perimeter with $z=0$. It is probably a very demanding technical requirement since the precision required is of the order of a wavelength. Errors would be insignificant for a very large mirror but not for a practical one. In principle it is possible to compensate for the mounting errors by applying voltage to the mirror at a price of a reduced dynamic range.

5. FINITE ELECTRODES

Until now we have assumed that the voltage applied to the mirror has a continuous distribution. This is technically impossible since the electrodes are of finite size. We shall not try to examine this in a fully rigorous way, but in a way which shall give us some insight.

We shall assume that the wave front curvature is measured spatially on a very large periodic array of sampling detectors (averaging over an area equivalent to that of a piezoelectric element) and then reconstructed by circular piezoelectric elements. If we neglect aliasing effects and utilize the Poisson equation obeyed by the mirror, then we find that the correction of the n th radial order (amount of rms error related to this order which can be removed) is given by:

$$0.0046 \left(\frac{D}{r_0} \right)^{\frac{5}{3}} (n+1) \int_0^\infty dk k^{-\frac{8}{3}} \left[\frac{J_{n+1}(2\pi k)}{k} \right]^2 \left[\frac{2J_1(2\pi k/x)}{(2\pi k/x)} \right]^4 \quad (24)$$

where $x = D/d$ and D is the diameter of the aperture. The number of electrodes is approximately

x^2 . By taking the limits of integration from zero to infinity we neglect any inner and outer turbulence scale considerations.

In Fig. 2 we plot the correction as the ratio of the removed wave front error relative to the full error contained in each aberration order. We should stress that these results are obtained for the case of matching ordered arrays of sampling detectors and reconstructing bimorph electrodes. A geometrical configuration designed specifically for the correction of low-order aberrations could achieve better results with less electrodes¹⁶

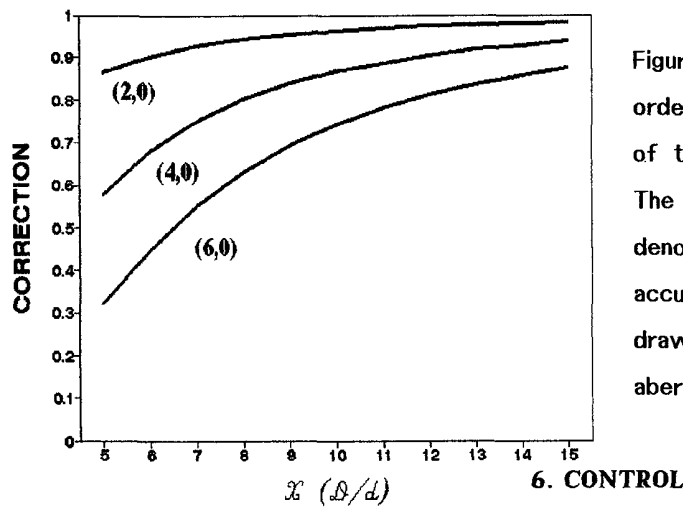


Figure 2. Correction of the first isotropic orders (approximate treatment). x is the ratio of the optical diameter to the electrode size. The Zernike radial and azimuthal orders are denoted by (n,m) . The calculation is more accurate for higher x values. The correction is drawn relative to the full correction (no aberrations) for each order.

Some practical aspects of the bimorph mirror and its possible coupling to a curvature sensor (and other) were discussed. It seems possible to attain a high level of correction, up to the fourth Zernike radial order, by using a mirror with about 100 electrodes on a rectangular grid. Overall mean error can be decreased dramatically by much fewer electrodes but will leave the higher aberration orders uncorrected.

The coupling of the bimorph mirror and the curvature sensor must be supplemented by corrections to the error terms computed above. This is done by a computational stage between the sensor and adaptive mirror. It is also possible to use the bimorph mirror with a slope sensor because the Zernike expansion of the wave front can be derived easily from the slopes¹⁷. A suggested strategy is to derive the Zernike decomposition of the wave front and then apply the appropriate voltage distribution to the mirror (including error corrections). The correction is done up to the term which is corrected to our satisfaction.

This algorithm can be represented in matrix form:

$$\mathbf{v} = \mathbf{M D s} \quad (25)$$

where \mathbf{v} is the vector of voltages applied to the mirror electrodes, \mathbf{s} is the vector of curvature or slopes signals, \mathbf{D} is the matrix which yields the Zernike expansion coefficients and \mathbf{M} is the matrix for the voltage distribution. \mathbf{M} can be computed analytically using the formulas derived above. This is done basically by using Eq. 7 and then taking into account the need to compensate for induced errors in Eqs. 19, 28. Finally, \mathbf{MD} can be combined into one matrix which can be pre-calculated for faster application. This interaction matrix can be measured experimentally¹⁴. The above work helps clarify the source of the off-diagonal terms so as to assist in designing better detector/bimorph electrode configurations.

7. EXPERIMENT

We built a number of bimorph mirrors and tested them. We used silicon wafers (from the electronics industry) for mirrors, and glued to them pieces of lead zirconium titanate. The silicon wafers were chosen to be conductive, and of optical quality on at least one surface. Typical thickness is $250\mu\text{m}$ to $500\mu\text{m}$ and diameter is 100 to 150 mm. One side was aluminized to serve as a reflective surface. The piezoelectric pieces are usually $250\mu\text{m}$ thick, and are round or square of dimension 10 to 15 mm. (It is not practical to have large piezoelectric elements because they are extremely fragile.) Leaving a few centimeters free on the rim, it is possible to pack a few tens of elements in the mirror. We have reached 61 elements in a hexagonal structure, and are now trying square elements with the same density. The areas between the elements cannot be deformed, so that it is better to minimize them by using square elements. Thermal effects have to be accounted for (it takes approximately 1V to correct for bending caused by 1K).

The voltage response of these mirrors is rather good - approximately $1\mu\text{m}$ to 10V inside each element. However, the structure tends to oscillate easily and hence has to be controlled very tightly using a servo system that is more complex than that of the standard piston mirror. The mirror is controlled by a personal computer holding a card with a bank of digital to analog converters, at a voltage range of $\pm 20\text{V}$.

We also experimented with a tip-tilt mirror (Fig. 3). Such a mirror is thick, so as not to suffer surface deformations. Four bimorph piezoelectric elements at the four sides of the mirror are attached to a frame with a flexible contact. Every two opposite bimorphs bend at opposite curvatures, to create an S shape. The bimorphs can be either glass-PZT, where the glass may be one piece with mirror, or two PZTs back to back.

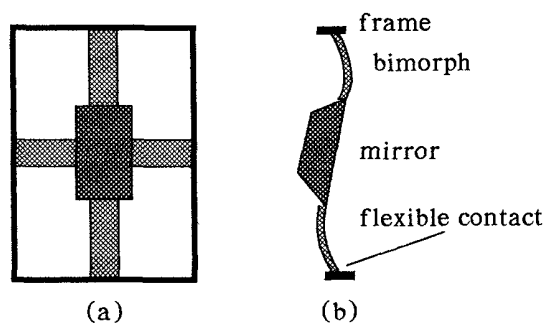


Fig. 3. (a) Tip-tilt mirror is constructed of thick mirror held by four bimorphs to a rigid frame. (b) When opposite bimorphs bend in opposite curvature, the mirror tilts in this direction.

ACKNOWLEDGEMENTS

The support of the Israeli Ministry of Science and Infrastructure is greatly appreciated. Support was also provided by the Goldberg Foundation, Technion, and by the Jet Propulsion Laboratory, California Institute of Technology.

REFERENCES

1. C. Schwartz, E.N. Ribak, and S.G. Lipson, "Bimorph adaptive mirrors and curvature sensing", *J. Opt. Soc. Am. A* **11**, in print (1994).
2. E. Steinhaus and S.G. Lipson, "Bimorph piezoelectric flexible mirror", *J. Opt. Soc. Am.* **69**, 478-481 (1979).
3. S.P. Timoshenko and S. Woinowsky-Kriger, *The theory of plates and shells*, 2nd ed., (McGraw-Hill, 1959), Chap. 4, Sect. 24, pp. 94-97.
4. S.A Kokorowsky, "analysis of adaptive optical elements made from piezoelectric bimorphs", *J. Opt. Soc. Am.* **69**, 181-187 (1979).
5. P.M. Morse and H. Feshbach, *Methods of theoretical physics*, (Mcgraw-Hill, 1953), Part 2, Chap. 10, pp. 1175-1215.
6. W.C. Young, *Roarks formulas for stress and strain*, 6th ed., (Mcgraw-Hill, 1989), Chap. 10, pp. 443-448.
7. P. Jagourel, P.Y. Madec and M. Sechaud, "Adaptive optics: A bimorph mirror for wave front correction", *SPIE 1237 (Amplitude and intensity spatial interferometry)*, 394-405 (1990).
8. F. Roddier, "A new concept in adaptive optics: curvature sensing and compensation", *Appl. Opt.* **27**, 1223-1225 (1988).

9. M. Born and E. Wolf, *Principles of optics*, 6th ed., (Pergamon Press, 1980), Appendix VII, pp. 767–772.
10. R.J. Noll, "Zernike polynomials and atmospheric turbulence", *J. Opt. Soc. Am.* **66**, 207–211 (1976).
11. J.Y. Wang and J.K. Markey, "Modal compensation of atmospheric turbulence phase distortion", *J. Opt. Soc. Am.* **68**, 78–87 (1978).
12. J.Y. Wang and D.E. Silva "Wave front interpretation with Zernike polynomials", *Appl. Opt.* **19**, 1510–1518 (1980).
13. D.L. Fried, "Optical resolution through a randomly inhomogeneous medium for very long and very short exposures", *J. Opt. Soc. Am.* **56**, 1372–1379 (1966).
14. N. Roddier, F. Roddier, "Curvature sensing and compensation: a computer simulation", *SPIE* **1114**, 92–96 (1989).
15. F. Roddier, "Wavefront curvature sensing and compensation in adaptive optics", *SPIE* **1487**, paper 8 (1990).
16. F. Roddier, M. Northcott, J. E. Graves, "A simple low-order adaptive optics system for near-infrared applications", *Pub. Astr. Soc. Pacific* **103**, 131–149 (1991).
17. R. Cubalchini, "Modal wave front estimation from phase derivative measurements", *J. Opt. Soc. Am.* **69**, 972–977 (1979) .